

## A study in the formation of $\text{Li}_7\text{La}_3\text{Zr}_2\text{O}_{12}$ as a Garnet-Type Ionic Conductor Synthesized by Flame Combustion.

Justin Roller<sup>1</sup>, Yang Wang<sup>2</sup> and Radenka Maric<sup>3</sup>

<sup>1</sup>. FEI Company, NA Nanoport, Portland, USA.

<sup>2</sup>. Department of Materials Science and Engineering at the University of Connecticut, Storrs, USA.

<sup>3</sup>. Department of Materials Science and Engineering and Department of Chemical and Biomolecular Engineering at the University of Connecticut, Storrs USA.

Solid-state lithium batteries capable of stability against chemical reaction with Li up to voltages higher than 5.5 V are considered a promising alternative to liquid or gel electrolytes that dominate the Li-battery market [1]. In addition, they can be deposited as thin film batteries (TFBs) and integrated directly onto microprocessor chips [2]. The transition to solid-state dry batteries will allow for miniaturization due to a decreased electrolyte thickness, easier handling during manufacture, increased safety due to the lack of a flammable electrolyte coupled with a wide electrochemical potential window, and by the reduced environmental impact of oxide based electrolytes.

$\text{Li}_7\text{La}_3\text{Zr}_2\text{O}_{12}$  (LLZ) is a garnet-type ionic conductor with bulk conductivities of  $3 \times 10^{-4} \text{ S cm}^{-1}$  at 25°C. In order to maintain such a high ionic conductivity the LLZ must crystallize in the cubic Ia-3d space group and not the preferred tetragonal  $I4_1/acd$  space group which has an ionic conductivity that is 2 orders of magnitude lower [3].

Reactive Spray Deposition Technology (RSDT) was the route used to manufacture LLZ in an open atmosphere one-step process as a thin film [4]. In order to understand the mechanisms of nanoparticle formation, ensure complete precursor conversion, study the effect of process parameters on crystallinity, and map the elemental distributions of lanthanum and zirconium, a STEM and TEM study was undertaken. TEM grids were used to sample forming nanoparticles under various processing conditions such as fuel flow rate and equivalence ratios. In addition, films were deposited on various substrates and then subjected to annealing temperatures to examine the resulting morphology and crystal structure.

The images and maps displayed in Figures 1-3 were obtained from samples prepared by wiping-off a portion of thin film deposited onto an Aluchrome YHf alloy and then sonicating the wipe in isopropanol (IPA). The IPA was then pipetted onto a 400 mesh grid having an ultrathin carbon film supported on a lacey film. All images were acquired on an FEI 200 kV Metrios TEM equipped with ChemiSTEM™ technology (X-FEG source and Super-X EDS). Figure 1 shows a 2  $\mu\text{m}$  field of view (FOV) HAADF image and highlights the Z-contrast of the La (Z=57) and Zr (Z=40) relative to the lacey and thin film carbon. The TEM image and accompanied diffraction pattern (DP) highlight the thickness and diffraction contrast of the nanoparticle grains. The randomly oriented particles contribute to the polycrystalline spots observed in the DP. Figure 2 is a Super-X EDS map of the elements present. The La and Zr are distributed as circular particles ranging in diameter from 20-130 nm. In addition, there are areas where the La and Zr that are not circular, but exist as smaller clustered particles. This indicates different mechanisms of precursor conversion in the flame. The O is co-located with the La/Zr but also exists in other areas. Figure 3 highlights an area where both the nanoparticles and the clusters are present.

## References:

- [1] R Murugan, V Thangadurai, and W. Weppner, *Angew. Chem. Int. Ed.* **46** (2007) p. 7778.  
 [2] J Tan and A Tiwari, *Journal of the Electrochemical Society* **1**(6) (2012), p. Q57.  
 [3] Y Wang and W Lei, *Journal of Power Sources* **275** (2015), p.612.  
 [4] J Roller, J Renner, H Yu et al., *Journal of Power Sources* **271** (2014), p. 366.

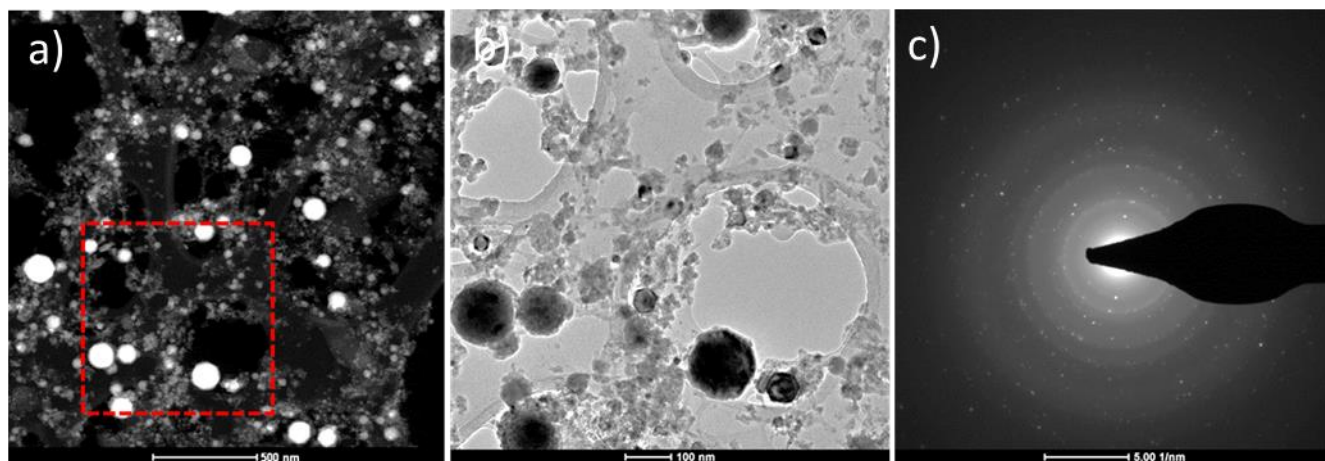


**Figure 1.** a) HAADF image with large 2  $\mu\text{m}$  FOV of LLZ nanoparticles and clustered areas. b) Same area imaged in bright field TEM with the associated c) diffraction pattern.

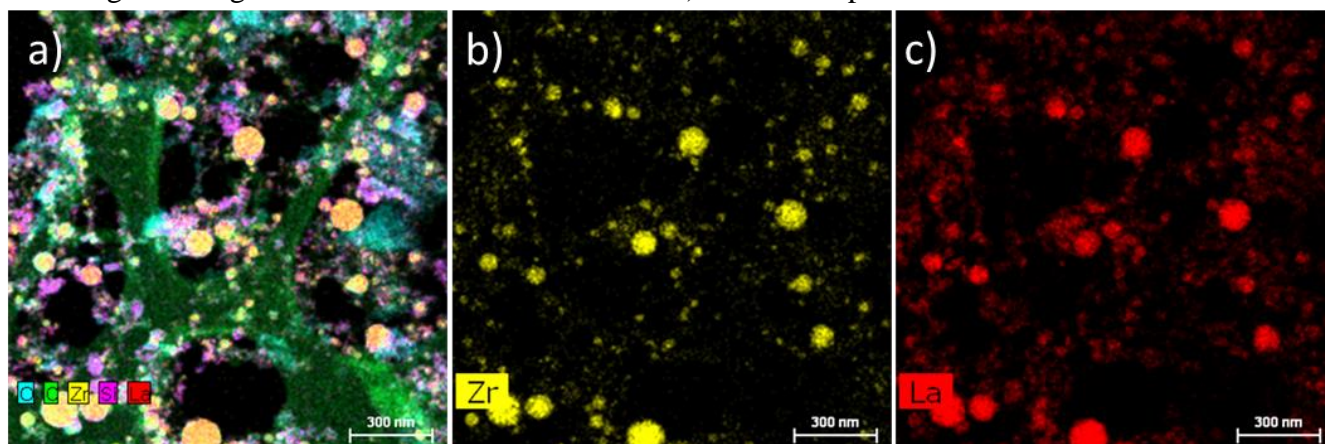


**Figure 2.** Super-X EDS maps of LLZ highlighting the elemental distribution of Zr and La in the nanoparticles and clusters.

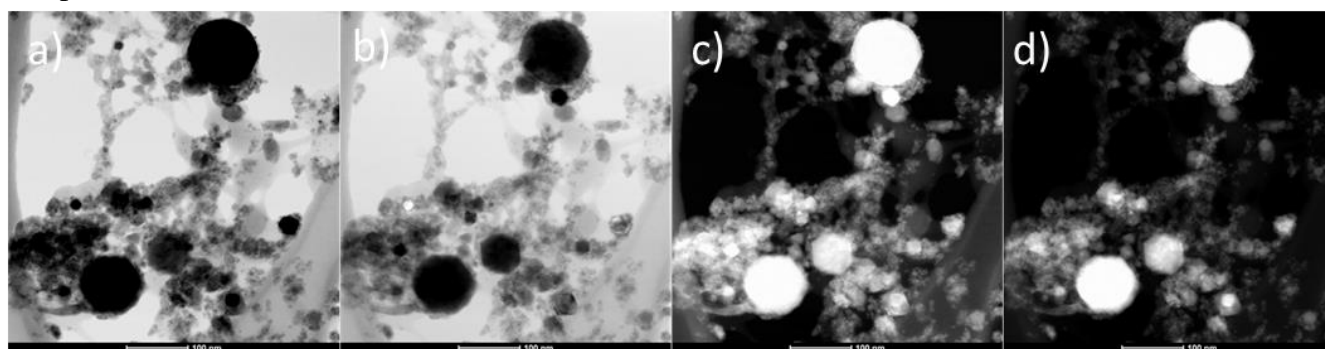


**Figure 3.** Simultaneous acquisition of a) bright field, b) annular bright field, c) dark field, and d) HAADF images of LLZ nanoparticles and cluster areas.